DOI: 10.55415/deep-2022-0055.v1

Biothiol-Triggered Hydrogen Sulfide (H_2S) Release from Near-Infrared Fluorescence H_2S Donor for Promoting Cutaneous Wound Healing

Xinyue Zhao[a,#], Mengbin Ding[c,#], Lulu Ning[d], Fang Yuan[a], Jingchao Li[c], Yuan Guo[a], Yuguang Mu[e], Jianjian Zhang[a,b,*]

[a] Key Laboratory of Synthetic and Natural Functional Molecule Chemistry of Ministry of Education, Key Lab of Modern Separation Science in Shaanxi Province, College of Chemistry and Materials Science, Northwest University, Xi'an, Shaanxi 710127, P. R. China

[b] Qinghai Provincial Key Laboratory of Salt Lake Resources Chemistry, Xining, 810008, P. R. China

[c] Shanghai Engineering Research Center of Nano-Biomaterials and Regenerative Medicine, College of Biological Science and Medical Engineering, Donghua University, Shanghai 201620, China

[d] Shaanxi Provincial Key Laboratory of Papermaking Technology and Specialty Paper Development, College of Bioresources Chemical and Materials Engineering, Shaanxi University of Science & Technology, Xi'an 710021, P. R. China

[e] School of Biological Sciences, Nanyang Technological University, 60 Nanyang Drive, Singapore 637551, Singapore

[#] These authors contributed equally to this work.

[*] Correspondence: orcid.org/0000-0002-5220-1280; Email: zhangjj@nwu.edu.cn (J. Zhang)

Abstract

Hydrogen sulfide (H_2S) plays crucial roles in antioxidation, anti-inflammation, and cytoprotection. Despite the great progress in the design and synthesis of activatable H_2S donors, high-precision detection and imaging of released H_2S in living systems is still an outstanding issue. In this study, a biothiol-activated near-infrared (NIR) fluorescent H_2S donor **PRO-ST** for real-time visualization of H_2S release is developed. **PRO-ST,** consisting of a dicyanoisophorone-based NIR fluorescence moiety (TCOO), a biothiol-trigger moiety (4-isothiocyanate benzyl alcohol), and a sulfur-source group (thiophosgene), is characterized by large NIR fluorescence enhancement (45-fold), outstanding H_2S release efficiency (73%), prominent controllable H_2S release (60 min) and excellent cell compatibility. The distinctive features render **PRO-ST** capable of visualizing H_2S release in cells, zebrafish, and mice. Moreover, **PRO-ST** has exhibited excellent performance of real-time anti-inflammation and wound healing enhancement in biological systems, which has been confirmed by *in-situ* visualization of H_2S release. The versatile **PRO-ST** provides possible and effective solution to the detection and visualization of H_2S release, which

DOI: 10.55415/deep-2022-0055.v1

will benefit the comprehension of underlying mechanisms of wound healing and the optimization of interventional therapy.

Keywords: H_2S donor; Biothiol-activated; Anti-inflammatory; Wound healing.

1. INTRODUCTION

Traumatic skin defects are associated with serious health problems and may deteriorate into lethal trauma without proper regeneration. Hence, the repair of skin tissue trauma is essential to reduce the suffering and prolong the life expectancy of patients.[1, 2] As a continuous, overlapping, and highly coordinated multi-tissue dynamic process, wound healing falls into three stages: inflammation, fibrous tissue hyperplasia, and matrix remodeling.[3, 4] In the begging of wound healing, the stress response from within triggers a severe inflammatory reaction in the body. Meanwhile, the overexpression of cytokines such as CRP (C-reactive protein), IL-6 (interleukin-6), and reactive oxygen free radicals has been activated by the dysregulation of multiple intracellular signaling pathways, which causes systemic inflammatory response syndrome (SIRS).[5] It has been shown that moderate inflammatory response is capable of protecting the wound and promoting wound healing. Whereas, excessive inflammatory response can lead to immune dysfunction, which inhibits wound healing and even causes life-threatening problems to the patient.[6, 7] Hence, it is imperative to design safe, effective and feasible strategies to accelerate wound healing, with a focus on balancing the immune response and regulating the inflammatory pathway.

H_2S, distributing in almost every living organ system, plays a significant role in different pathologies and disease states .[8-12] H_2S exhibits multiple functions such as protecting the central nervous system, mitigating oxidative stress in the cardiovascular system, and modulating blood pressure homeostasis.[13] Moreover, H_2S plays a part in diverse effects such as anti-oxidant, anti-inflammatory, and cytoprotection due to its direct interaction with major signaling pathways related with various disease states.[14-17] Therefore, developing molecules possessing the ability to regulate H_2S level at wound can facilitate the control of inflammatory response and

DOI: 10.55415/deep-2022-0055.v1

promote early wound healing. Furthermore, the development and research of small molecule H_2S donors are crucial to understand the underlying mechanisms of wound healing, which may benefit the optimization of interventional therapy.

Although great efforts have been dedicated to the design and application of activatable H_2S donors,[18-20] the visualization and accurate detection of released H_2S in living systems still remain a vital challenge ascribing to the inconvenience and insufficient sensitivities of many traditional analytical technologies, such as electrochemistry,[21, 22] gas chromatography,[23, 24] and colorimetry.[25, 26] In recent years, fluorescence imaging has engaged attentions of researchers because of its high selectivity, high sensitivity, convenience, less invasiveness, and real-time imaging capability.[27-40] Excellent H_2S releasing efficiency with long wavelength fluorescence emission and capability of visualizing H_2S release are prerequisites to be a competent H_2S donors. Several H_2S donors with intrinsic fluorescent signal changes have been reported, which can be activated by various exogenous or endogenous stimuli such as light,[41-43] pH modulation,[44, 45] enzymes,[46, 47] cellular thiols,[48-51] and reactive oxygen species (ROS)[52, 53] and release H_2S. However, some of them have drawbacks such as uncontrollable H_2S release, low H_2S releasing efficiency, and short wavelength emission, which are unsuitable for application in living systems to treat related diseases. Recently, a Cys-triggered NIR fluorescent H_2S donor was developed by our group,[54] which was suitable to be applied for anti-inflammation in living cells. However, its main fluorescence products were not generated in the same pathway as H_2S and the observed fluorescence was not correlated with H_2S concentration in some cases, which fails to realize the precise detection of H_2S.

Herein, we developed a biothiol-activated NIR fluorescence H_2S donor **PRO-ST** (Figure 1a) for real-time visualization of H_2S release. **PRO-ST** consists of a dicyanoisophorone-based NIR fluorescence moiety (TCOO), a biothiol-trigger moiety (4-isothiocyanate benzyl alcohol), and a sulfur-source group (thiophosgene) (Figure 1b). The optical response of **PRO-ST** under biothiol-induced cleavage has been evaluated and the reaction mechanism underlying H_2S release has been verified with

DOI: 10.55415/deep-2022-0055.v1

the kinetics and release efficiency of H_2S. The anti-inflammatory and the wound healing abilities of **PRO-ST** have also been studied in LPS-induced inflammatory macrophages and in mice, respectively.

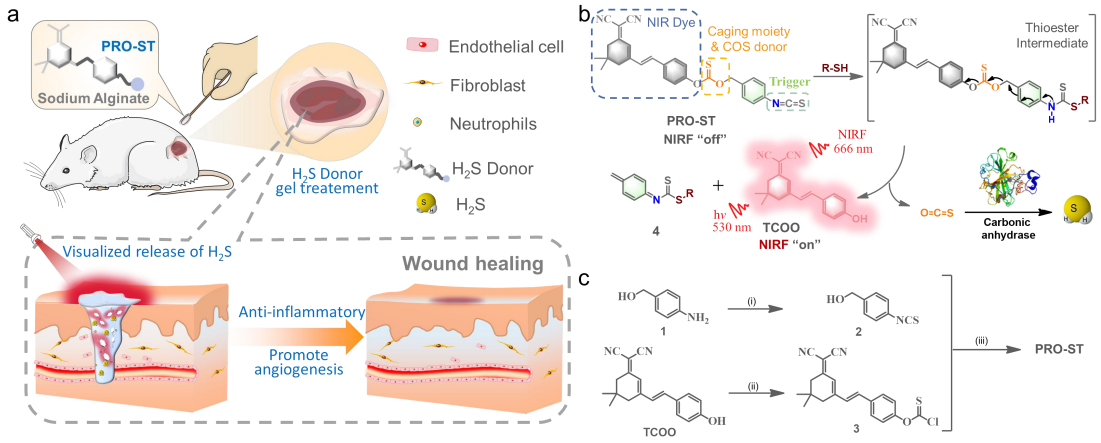

Figure 1. a) Schematic illustration of the design of **PRO-ST** for visualizing H_2S release and promoting wound healing via inhibiting inflammation. b) Schematic diagram of the mechanism of boithiols-activated COS/H_2S releasing with fluorescence response from **PRO-ST**. c) Synthesis route of **PRO-ST**. (i) thiophosgene, anhydrous CH_2Cl_2, room temperature, 0.5 h; (ii) thiophosgene, anhydrous THF, KOH, room temperature, 1 h; (iii) 4-dimethylaminopyridine (DMAP), anhydrous CH_2Cl_2, room temperature, 10 min.

2. RESULTS AND DISCUSSION

The synthesis route of **PRO-ST** was presented in Figure 1c. (4-isothiocyanatophenyl)methanol was synthesized by stirring (4-aminophenyl)methanol **1** and thiophosgene in a dichloromethane solution. The middle component **3** was obtained from TCOO by caging the oxygen atom with a thiochloroformate group. Compound **3** was then reacted with **2** in the presence of DMAP to give the desired H_2S donor **PRO-ST** (Figure S1-S8 and Methods, Supporting Information).

To evaluate the fluorescence response induced by biothiol-trigger cleavage, the fluorescence spectral properties of **PRO-ST** were investigated before and after the treatment of GSH, Cys, and Hcy, respectively. As shown in Figure 2a, **PRO-ST** intrinsically had hypofluorescence with a low fluorescence quantum yield (Φ_F = 0.008). This phenomenon can be attributed to strong electron-withdrawing property of carbon-sulfur double bond in **PRO-ST**, which diminished the electron-donating ability of the aromatic hydroxy group and finally quenched the fluorescence of TCOO. Upon addition of GSH (20 equiv), the fluorescence intensity of **PRO-ST** at 666 nm

DOI: 10.55415/deep-2022-0055.v1

was increased by 45~fold compared with its initial state. In addition, a distinct Stokes shift of 136 nm was also observed. Similarly, the addition of Cys and Hcy could also significantly enhance the fluorescence of **PRO-ST** by 37-fold and 17-fold, respectively. The turn-on fluorescence responses may be resulted from the rapid nucleophilic attack on the isothiocyanate in **PRO-ST** by -SH of biothiol, followed by intramolecular 1, 6-elimination with the fluorophore (TCOO) and COS released (Figure 1b).

To confirm our assumption, mass spectrum analysis was performed, which showed that **PRO-ST** was decomposed into expected TCOO (*m/z*, 289.2), nucleophilic addition-elimination quinones product (*m/z*, 309.1), and thioester intermediate (*m/z*, 659.1) after being treated with NAC (a compound with an acetyl group attached to the amino group of cysteine) (Figure S9, Supporting Information). Moreover, the mass spectrum of **PRO-ST** revealed the same results that the common fluorophore TCOO and the corresponding nucleophilic addition-elimination quinones product (*m/z*, 453.1, 267.0, and 281.0) were generated after reacting with GSH, Cys, and Hcy, respectively (Figure S10-12, Supporting Information). To further prove the role of -SH in biological thiols, *β*-mercaptoethanol (*β*-ME), NAC, Cystine, and Cysteamine with a molecular structure similar to GSH, Cys, and Hcy were selected as control compounds. it has been observed that the compounds containing the -SH group could activate **PRO-ST** to produce a fluorescent signal, whereas the compounds containing the amino group without -SH could not (Figure S13, Supporting Information), which indicated that -SH participates in nucleophilic attack on isothiocyanates rather than amino group. Therefore, fluorescent signals of **PRO-ST** are activated by the -SH group in biological thiols through preferentially attacking the isothiocyanate to occur in nucleophilic addition, which is consistent with the mechanism we hypothesized.

The selectivity of **PRO-ST** towards biothiols (GSH, Cys, Hcy) against various biological relevant species, such as H_2S, BSA, amino acids (Arg, Gly, Val, Ser, Leu, Asn, Asp, His, Pro, Tyr, Thr, Glu, Lys, Phe, Met, Ile), metal ions (Ca^{2+}, Na^{+}, Mg^{2+}, K^{+}, Zn^{2+}, Cu^{2+}, Al^{3+}, Fe^{3+} Hg^{2+}, and Fe^{2+}), and RONSs ($^1O_2$, $O_2^{\cdot-}$, H_2O_2, ClO^{-}, ·OH,

DOI: 10.55415/deep-2022-0055.v1

$ONOO^-$, NO_2^-), was investigated (Figure 2b and S14 Supporting Information). None of them could induce significant fluorescence changes for **PRO-ST**, indicating the high selectivity of **PRO-ST** to biothiols. The changes in the fluorescence spectra of **PRO-ST** toward biothiols allow for quantification of the signals based on the fluorescence intensity at 666 nm (Figure S15-17, Supporting Information). Good linear correlations between the fluorescence signal and the concentration of GSH, Cys, and Hcy were observed with the limit of detection (LOD) of 28.1, 41.4, and 33.2 nM, respectively (Figure 2c). The kinetics of GSH-, Cys-, and Hcy-induced optical changes of **PRO-ST** were also investigated (Figure 2d) and the fluorescence intensity of **PRO-ST** at 666 nm reached a plateau in about 60 min, which suggested that **PRO-ST** could be activated by biothiols slowly. These data proved that **PRO-ST** had a specific and controllable fluorescence response toward biothiols.

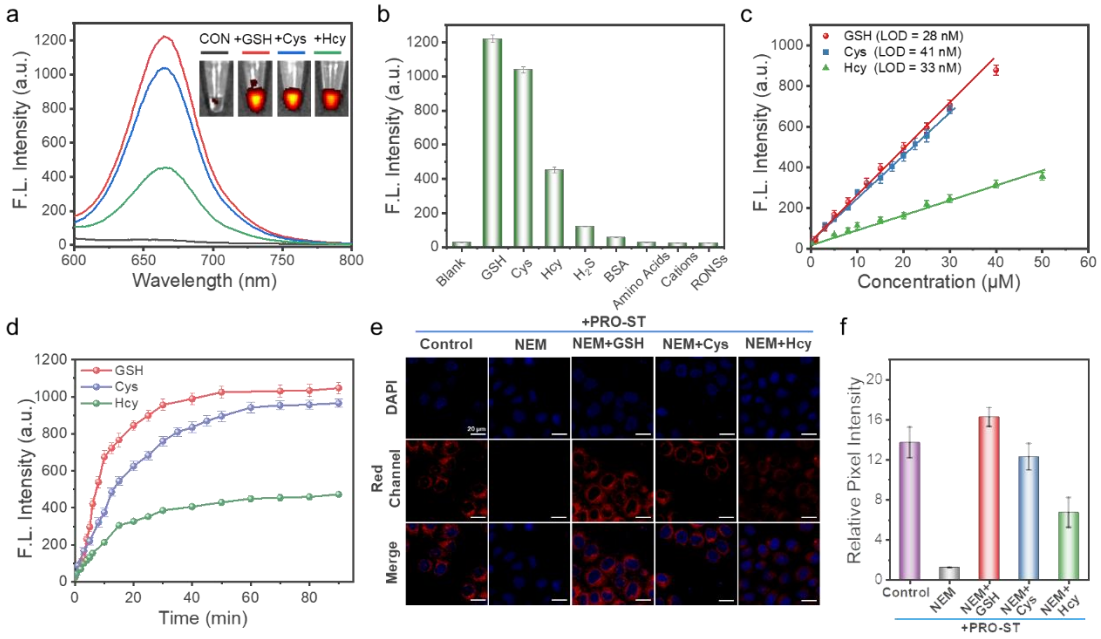

Figure 2. a) Fluorescence spectra of **PRO-ST** in the absence or presence of GSH/Cys/Hcy under aqueous DMF/PBS solutions (pH 7.4, 20 mM, *v/v*, 3/7). Inset: the corresponding fluorescence imaging of **PRO-ST** upon addition of GSH/Cys/Hcy acquired at 666 nm with the IVIS spectrum imaging system. b) Fluorescence intensity of **PRO-ST** at 666 nm toward different substances (200 μM) including GSH, Cys, Hcy, H_2S, BSA, amino acids, cations, and RONSs. c) Linear correlation between the fluorescence intensity of **PRO-ST** and varying concentrations of GSH/Cys/Hcy. d) Time-dependent fluorescence intensity of **PRO-ST** upon addition of GSH/Cys/Hcy. e) Confocal fluorescence microscopy images of RAW-246.7 cells incubated with **PRO-ST**. (first column) untreated cells; (second column) cells preincubated with NEM; (third-fifth column) NEM-

DOI: 10.55415/deep-2022-0055.v1

preincubated cells were intreated with GSH/Cys/Hcy, respectively. f) Relative fluorescence intensity of the corresponding fluorescence images in e). **Note:** the concentration of **PRO-ST**, C-7AZ, and biothiols was 10 μM, 3 μM, and 200 μM, respectively, when there was no special mark.

To verify whether biothiols in cells could activate **PRO-ST** to release fluorophore TCOO, murine macrophage (RAW 264.7) cells treated with **PRO-ST** were imaged. Before the bioimaging experiment, cell viability studies were performed with **PRO-ST** and its reaction product TCOO, which showed that when the concentration of **PRO-ST** and TCOO increased to 50 μM, the survival rate of RAW 264.7 cells still reached more than 75% (Figure S18, Supporting Information). After being incubated with **PRO-ST**, the cytoplasm of the cells exhibited an obvious red fluorescence. However, when pretreated with N-Ethylmaleimide (NEM), an effective sulfhydryl scavenger,[55] the cytoplasm of the cells displayed a faint red fluorescence. Further quantification demonstrated that the fluorescence intensity of NEM-preincubated cells was 9% lower than that of unpreincubated cells (Figure 2f). In addition, when NEM-pretreated RAW 246.7 cells were cultured with exogenous GSH, Cys, and Hcy, respectively, recovery of strong fluorescence signals was observed. These results suggest that the intense fluorescence in RAW 246.7 cell cytoplasm was induced by the intracellular biothiols, which triggered the activation of **PRO-ST**. Moreover, the biocompatibility of **PRO-ST** *in vivo* was also confirmed in zebrafish and mouse imaging experiments (Figure S19-20, Supporting Information).

As shown in Scheme 1A, COS, released from **PRO-ST** in the presence of biothiols, can be converted to H_2S by carbonic anhydrase (CA).[56] To verify the above mechanism, C-7AZ, an H_2S-responsive fluorescence probe,[57] was used to detect H_2S (Figure 3a and S21, Supporting Information). As shown in Figure 3a, when C-7AZ was added to the reaction solution, no significant fluorescence intensity increase at 450 nm was observed in the absence of CA compared with the control group (λ_{ex} = 350 nm). However, the fluorescence intensity of the GSH group in the presence of CA was obviously enhanced, of which the fluorescence intensity was about 10-fold higher than that of the control group. Similarly, compared with the control group, the fluorescence intensity of the Cys and Hcy groups were increased by

DOI: 10.55415/deep-2022-0055.v1

8- and 5-fold, respectively. These results demonstrated that the release of H_2S from **PRO-ST** depend on the generation of COS and the catalysis of CA.

To investigate the release efficiency of H_2S from **PRO-ST** triggered by biothiols, the kinetic study using methylene blue (MB) assay was performed.[58] At 667 nm, the absorption intensity of MB solution increased gradually in the presence of CA and reached a plateau in about 2 h after incubation of **PRO-ST** with GSH (Figure 3b). Moreover, 18.2 μM of H_2S was measured with 73% releasing efficiency according to the calibration curve between MB and H_2S (Figure S22 and S23, Supporting Information). It has been found that Cys and Hcy also could trigger **PRO-ST** to release H_2S (14.1 and 9.0 μM) at the same condition with moderate releasing efficiency of 57% and 36%, respectively (Figure S24 and S25, Supporting Information). Therefore, these results indicated that **PRO-ST** would be a promising candidate for the highly efficient and controllable release of H_2S.

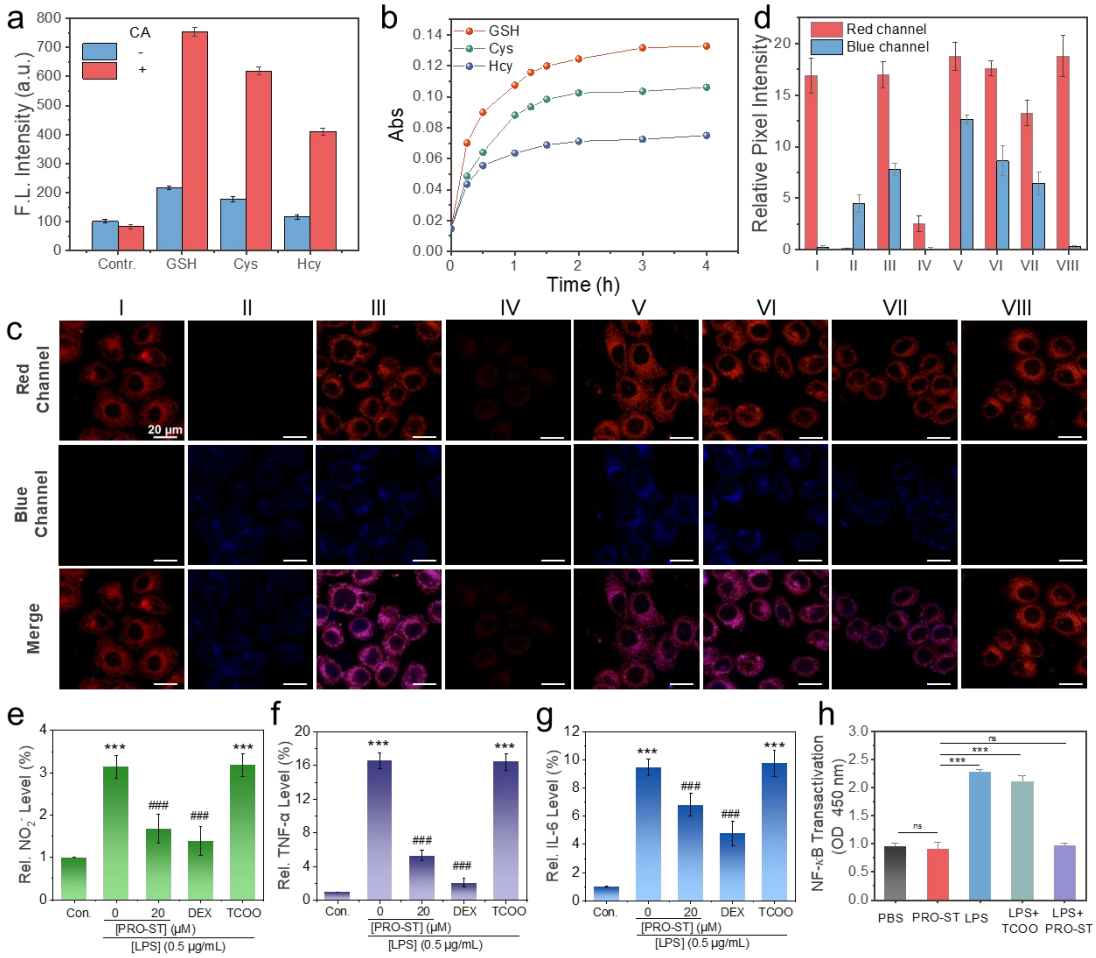

Figure 3. a) Fluorescence intensity of C-7AZ in the presence of **PRO-ST**, biothiols, and with or

DOI: 10.55415/deep-2022-0055.v1

without CA, λ_{ex} = 350 nm, λ_{em} = 450 nm. b) Time-dependent absorption intensity of MB reacted with **PRO-ST** (25 μM), GSH/Cys/Hcy (250 μM) and CA (25 μg/mL), λ_{abs} = 667 nm. c) Confocal fluorescence microscopy images of RAW 246.7 cells. (Ⅰ) Cells treated with **PRO-ST**. (Ⅱ) Cells treated with C-7AZ; (Ⅲ) Cells treated with **PRO-ST** and C-7A; (Ⅳ) NEM-pretreated Cells were incubated with **PRO-S** and C-7AZ; (Ⅴ-VII) NEM-pretreated Cells were incubated with GSH, Cys, and Hcy, respectively, then incubated with **PRO-ST** and C-7AZ, in turn. (Ⅷ) Cells were incubated with AAA (2.5 μM), **PRO-ST** and C-7A, in turn. Blue channel: λ_{ex}=405 nm, λ_{em}= 450 ± 20 nm; Red channel: λ_{ex}=514 nm, λ_{em}=660 ± 30 nm. d) Relative fluorescence intensity of the corresponding fluorescence images in c). Effects of **PRO-ST** on nitrite (e), TNF-α (f), and IL-6 (g) in LPS-pretreated RAW264.7 cells. Results are expressed as mean, SD (n = 3), $^{###}P < 0.001$ vs the 0 μM **PRO-ST** group, ***P < 0.001 vs the control group. h) **PRO-ST** suppressed NF-κB transactivation. **Note:** The concentration of **PRO-ST**, C-7AZ, and biothiols was 10 μM, 3 μM, and 200 μM, respectively, when there was no special mark. Results are expressed as mean, SD (n = 3), $^{###}P <$ ***P < 0.001 vs the **PRO-ST** group, ^{ns}No statistically significant difference.

To assess the capability of **PRO-ST** to release H_2S in the cellular environment, C-7AZ was introduced to verify the release of H_2S,[57] which could be validated by fluorescence enhancement in the blue channel. As shown in Figures 3c and 3d, RAW 246.7 cells solely treated with C-7AZ showed inconspicuous fluorescence in the blue channel, which might be caused by endogenous H_2S (column II). However, after being treated with **PRO-ST** and C-7AZ, both the red channel and blue channel showed obvious enhancement fluorescence signals (column III). Moreover, preincubated with a potent sulfhydryl scavenger NEM, the fluorescence of the cells at both channels decreased significantly when **PRO-ST** and C-7AZ were added successively (column IV). Whereas, when the NEM-pretreated cells were incubated with exogenous GSH, Cys, and Hcy, respectively, the fluorescence of the cells at both channels were restored (columns V, VI, and VII). These results suggest that biothiols are one of the major factors responsible for the changes in cellular fluorescence signals. In order to validate the necessity of CA in the conversion from COS to H_2S,[56] RAW 246.7 cell was pretreated acetazolamide (AAA, a CA inhibitor[59]), **PRO-ST**, and C-7AZ successively. As shown in Figure 3c (VIII column), negligible fluorescence signals were observed only in blue channels, which were consistent with the previous results obtained in an aqueous solution (Figure 3a). These data thus confirmed the suitability of **PRO-ST** for controllable and visualized H_2S release in cells.

DOI: 10.55415/deep-2022-0055.v1

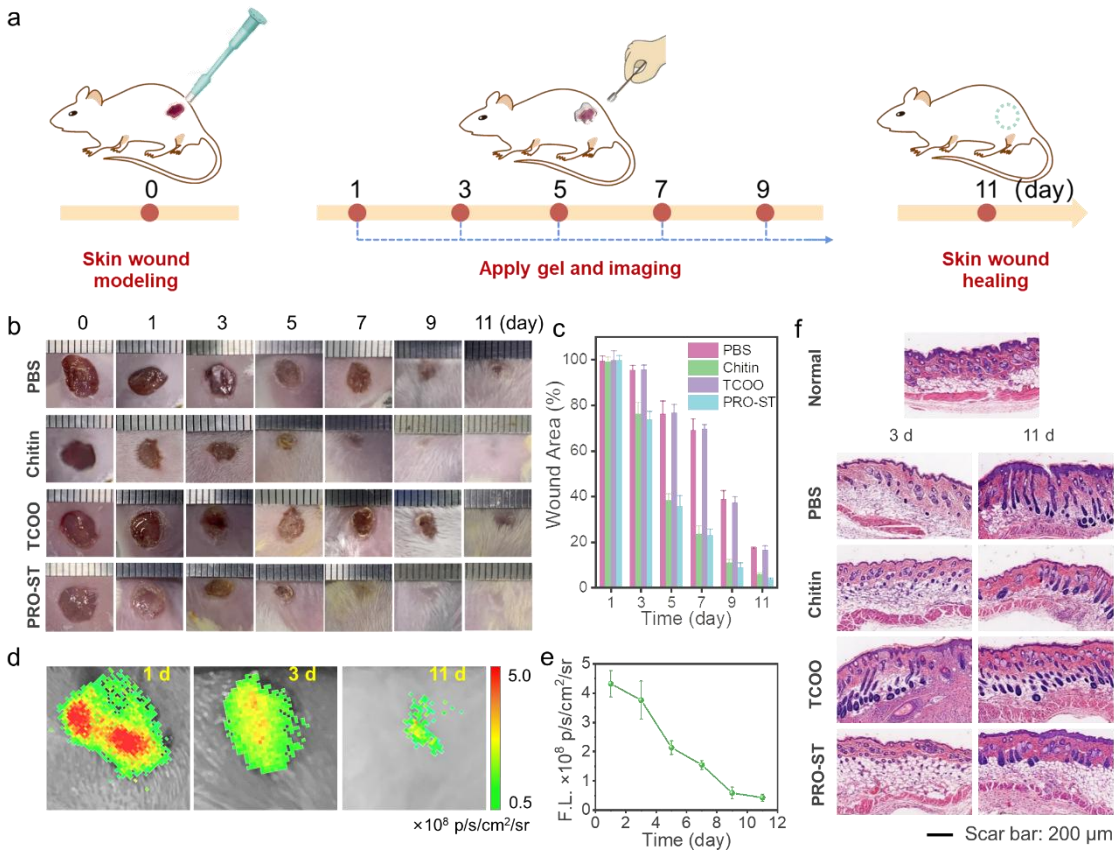

Figure 4. a) Schematic illustration of overall experiment utilizing **PRO-ST** sodium alginate gel for the therapy of cutaneous wound. b) Representative images of full-thickness cutaneous wounds at different time intervals treated with PBS buffer, Chitin gel, TCOO gel, and **PRO-ST** gel. c) Relative wound areas (% of day 0) of PBS buffer, Chitin gel, TCOO gel, and **PRO-ST** gel-treated groups on days 1, 3, 5, 7, 9, and 11 after injury. Statistical analysis was performed using one-way ANOVA. d) fluorescence imaging of the cutaneous wound of living mice, λ_{ex}=514 nm. e) Relative fluorescence intensity of the corresponding fluorescence images in d). f) Hematoxylin and eosin (H&E)-stained sections of healthy skin and wound tissues on day 3 and day 11 treated with PBS buffer, Chitin gel, TCOO gel, and **PRO-ST** gel, respectively. Scale bars: 200 μm.

Previous studies have verified that H_2S has anti-inflammatory effects at physiological concentrations. In addition to the mechanism underlying the release of H_2S, the anti-inflammatory effect of **PRO-ST** in RAW264.7 cells was further evaluated. Lipopolysaccharide (LPS), known as endotoxin,[60] was used to establish the cellular inflammation model. The introduction of LPS activates the upregulation of nuclear factor kappa-B (NF-*κ*b), a pleiotropic transcription factor that is linked to inflammation, through intracellular signaling pathways.[61] The activated NF-*κ*b induced the regulation of various cytokine inflammatory mediators, including TNF-α, NO_2^-, and cytokines IL-6, subsequently.[62] Appropriate concentration of H_2S can

DOI: 10.55415/deep-2022-0055.v1

effectively inhibit the activation of the NF-κB signaling pathway and regulate the excessive release of inflammatory mediators[15]. Therefore, the anti-inflammatory effect of **PRO-ST** has been evaluated based on the accumulation of NO_2^-, TNF-α, and IL-6 in LPS- exposed RAW 264.7 cells, which can be measured by Griess Reagent Kit and ELISA kit. As shown in Figure 3e-g, the LPS-exposed RAW264.7 cells present significant increases in the expression levels of NO_2^-, TNF-α, and IL-6 compared with the control group. When the LPS-incubated cells were treated with **PRO-ST**, accumulation of NO_2^-, TNF-α, and IL-6 was impaired significantly, which indicates good anti-inflammatory performance of PRO-ST. Similar inhibiting effect has also been observed in the positive control group (dexamethasone, DEX, an effective anti-inflammatory drug). It was worth noting that the LPS-pretreated cells incubated with byproducts TCOO were unable to inhibit LPS-induced production of NO_2^-, TNF-α, and IL-6, which indicated that H_2S released from **PRO-ST** played a crucial role in the anti-inflammatory effect.

The relationship between the accumulation of inflammatory mediators and NF-κB has been also evaluated. A 96-well ELISA kit was used for measuring the NF-*K*b DNA binding activity. As shown in Figure 3h, LPS-exposed cells displayed strongly upregulated nuclear translocation of NF-κB while **PRO-ST** alone hardly affected the translocation of NF-κB compared with the PBS group. Moreover, **PRO-ST** significantly suppressed LPS-induced NF-κB transactivation, indicating that the anti-inflammatory effect of **PRO-ST** may be achieved by blocking NF-κB transactivation.

A wealth of evidence suggested that wound healing involves complex processes such as inflammation, proliferation, and remodeling.[63] In chronic wounds, reducing the inflammatory response is considered an effective way to promote wound healing.[64] It has been reported that H_2S can effectively inhibit the excessive release of inflammatory mediators.[13] Hence, the wound healing effects of **PRO-ST** were evaluated in a murine full-thickness cutaneous wound model by periodical recording the conditions of wound contraction (Figure 4a). To better dress the wound, **PRO-ST** was gelled with sodium alginate, a natural polysaccharide serving as an excipient for pharmaceutical preparations with the stability, solubility, viscosity, and safety. As

DOI: 10.55415/deep-2022-0055.v1

shown in Figure 4b, the wound began to shrink from the edge over time in all experimental groups, which resulted from the body's natural self-healing capability. Moreover, in comparison with the control group treated with PBS buffer and TCOO-treated group, significantly accelerated wound closure was observed in mice applied with **PRO-ST** gel on the 3rd day of post-surgery, which had the same therapeutic effect as the Chitin-treated group (positive group). After 7 days of treatment, the wound area was smaller (Figure 4c), which exhibited that the wound was almost completely healed. In addition, fluorescence imaging experiments showed a significant decrease in fluorescence intensity with the increase of treatment days (Figures 4d and 4e), which demonstrated that **PRO-ST** was able to visualize the wound healing.

Controlling inflammation is a crucial step for wound healing. The hematoxylin and eosin (H&E) staining histological analyses were established (Figure 4f). On the 3rd day of post-surgery, an abundance of inflammatory cell infiltration was found in the negative control group treated with PBS buffer and TCOO gel. While the **PRO-ST** gel group, as well as the positive control group treated with chitin gel, exhibited less inflammatory cell infiltration compared with the negative control group treated with PBS, presumably due to the anti-inflammatory effect of H_2S. Furthermore, on the 11th day of post-surgery, an abundance of multinucleate giant cells and neo-epidermis was exhibited in the **PRO-ST** gel group with its histomorphology similar to that of normal skin, which has also been observed in the chitin gel group. In contrast, no significant improvement was observed in the negative control group. The histological results demonstrate that the H_2S released from **PRO-ST** promotes re-epithelialization and epidermal repair occurring in the wound area.

3. CONCLUSION

In summary, we have developed a biothiol-activated NIR fluorescence H_2S donor **PRO-ST** for real-time visualization of H_2S release. Compared with the previously reported donor (Table S1, Supporting Information), **PRO-ST** was featured by controllable release of H_2S with controlled and higher efficiency (up to 73%)

DOI: 10.55415/deep-2022-0055.v1

Furthermore, **PRO-ST** managed to repair the deficiency of previous H_2S donor from which H_2S is not generated in the same path as the main fluorescent product. More importantly, **PRO-ST** can be activated by multiple biothiol stimulants to release H_2S, which avoids the excessive consumption of a single stimulant and keeps the local redox balance. Additionally, real-time anti-inflammation and *in-situ* wound-healing promoting capabilities have been achieved by **PRO-ST** in the biological system, which indicates that **PRO-ST** has potential application in the clinical treatment of skin trauma.

ACKNOWLEDGEMENTS

This work was supported by the National Natural Science Foundation of China (21904105, 22277098), Innovation Platform Construction Project for Key Laboratory of Salt Lake Resources Chemistry of Qinghai Province (2022-ZJ-Y06), Start-Up grant of Northwest University, Natural Science Basic Research Plan in Shaanxi Province of China (2021JQ-537)

CONFLICTS OF INTEREST

The authors declare no competing financial interest.

REFERENCES

[1] Kurita M, Araoka T, Hishida T, O'Keefe DD, Takahashi Y, Sakamoto A, et al.: In Vivo Reprogramming of Wound-Resident Cells Generates Skin Epithelial Tissue. *Nature* 2018, 561 (7722): 243-247.

[2] Gurtner GC, Werner S, Barrandon Y, Longaker MT: Wound Repair and Regeneration. *Nature* 2008, 453 (7193): 314-321.

[3] Gosain A, DiPietro LA: Aging and Wound Healing. *World Journal of Surgery* 2004, 28 (3): 321-326.

[4] Xue M, Jackson CJ: Extracellular Matrix Reorganization During Wound Healing and Its Impact on Abnormal Scarring. *Advances in Wound Care* 2015, 4 (3): 119-136.

[5] Guo S, DiPietro LA: Factors Affecting Wound Healing. *Journal of Dental Research* 2010, 89 (3): 219-229.

[6] Boniakowski AE, Kimball AS, Jacobs BN, Kunkel SL, Gallagher KA: Macrophage-Mediated Inflammation in Normal and Diabetic Wound Healing. *The Journal of Immunology* 2017, 199 (1): 17-24.

[7] Boniakowski AM, denDekker AD, Davis FM, Joshi A, Kimball AS, Schaller M, et al.: SIRT3 Regulates Macrophage-Mediated Inflammation in Diabetic Wound Repair. *Journal of Investigative Dermatology* 2019, 139 (12): 2528-2537.

[8] Zhang H, Yue X, Li W, Chen W, Wang Y, Li X, et al.: Selective and Discriminative Fluorescence Sensing of Cys, Hcy, GSH and H_2S with Concise and Distinct Signals. *Sensors and Actuators B: Chemical* 2021, 331: 129394.

DOI: 10.55415/deep-2022-0055.v1

[9] Hong J, Feng W, Feng G: Highly Selective Near-Infrared Fluorescent Probe with Rapid Response, Remarkable Large Stokes Shift and Bright Fluorescence for H_2S Detection in Living Cells and Animals. *Sensors and Actuators B: Chemical* 2018, 262: 837-844.

[10] Ou-Yang J, Jiang W, Tan K, Liu H, Li S, Liu J, et al.: Two-Photon Fluorescence Probe for Precisely Detecting Endogenous H_2S in Lysosome by Employing a Dual Lock System. *Sensors and Actuators B: Chemical* 2018, 260: 264-273.

[11] Wang C, Cheng X, Tan J, Ding Z, Wang W, Yuan D, et al.: Reductive Cleavage of C-C Bonds as a New Strategy for Turn-on Dual Fluorescence in Effective Sensing of H_2S. *Chemical Science* 2018, 9 (44): 8369-8374.

[12] Zhou S, Mou Y, Liu M, Du Q, Ali B, Ramprasad J, et al.: Insights into the Mechanism of Thiol-Triggered COS/H_2S Release from N-Dithiasuccinoyl Amines. *The Journal of Organic Chemistry* 2020, 85 (13): 8352-8359.

[13] Whiteman M, Li L, Rose P, Tan C, Parkinson DB, Moore PK: The Effect of Hydrogen Sulfide Donors on Lipopolysaccharide-Induced Formation of Inflammatory Mediators in Macrophages. *Antioxidants & Redox Signaling* 2010, 12 (10): 1147-1154.

[14] Zhao Y, Cerda Matthew M, Pluth MD: Fluorogenic Hydrogen Sulfide (H_2S) Donors Based on Sulfenyl Thiocarbonates Enable H_2S Tracking and Quantification. *Chemical Science* 2019, 10 (6): 1873-1878.

[15] Barresi E, Nesi G, Citi V, Piragine E, Piano I, Taliani S, et al.: Iminothioethers as Hydrogen Sulfide Donors: From the Gasotransmitter Release to the Vascular Effects. *Journal of Medicinal Chemistry* 2017, 60 (17): 7512-7523.

[16] Hu Y, Li X, Fang Y, Shi W, Li X, Chen W, et al.: Reactive Oxygen Species-Triggered Off-on Fluorescence Donor for Imaging Hydrogen Sulfide Delivery in Living Cells. *Chemical Science* 2019, 10 (33): 7690-7694.

[17] Hua W, Zhao J, Gou S: A Naphthalimide Derivative Can Release COS and Form H_2S in A Light-controlled Manner and Protect Cells Against ROS with Real-time Monitoring Ability. *Analyst* 2020, 145 (11): 3878-3884.

[18] Szabo C, Papapetropoulos A: International Union of Basic and Clinical Pharmacology. CII: Pharmacological Modulation of H_2S Levels: H_2S Donors and H_2S Biosynthesis Inhibitors. *Pharmacological Reviews* 2017, 69 (4): 497-564.

[19] Zhao Y, Biggs TD, Xian M: Hydrogen Sulfide (H_2S) Releasing Agents: Chemistry and Biological Applications. *Chemical Communications* 2014, 50 (80): 11788-11805.

[20] Corvino A, Frecentese F, Magli E, Perissutti E, Santagada V, Scognamiglio A, et al.: Trends in H_2S-Donors Chemistry and Their Effects in Cardiovascular Diseases. *Antioxidants* 2021, 10 (3): 429.

[21] Khan MAH, Rao MV, Li Q: Recent Advances in Electrochemical Sensors for Detecting Toxic Gases: NO_2, SO_2 and H_2S. *Sensors* 2019, 19 (4): 905.

[22] Xu T, Scafa N, Xu L, Zhou S, Abdullah Al-Ghanem K, Mahboob S, et al.: Electrochemical Hydrogen Sulfide Biosensors. *Analyst* 2016, 141 (4): 1185-1195.

[23] Vitvitsky V, Banerjee R: H_2S Analysis in Biological Samples using Gas Chromatography with Sulfur Chemiluminescence Detection. *Methods In Enzymology* 2015, 554: 111-123.

[24] Ubuka T, Abe T, Kajikawa R, Morino K: Determination of Hydrogen Sulfide and Acid-Labile Sulfur in Animal Tissues by Gas Chromatography and Ion Chromatography. *Journal of Chromatography B: Biomedical Sciences and Applications* 2001, 757 (1): 31-37.

[25] Cha J, Kim D, Choi S, Koo W, Kim I: Sub-Parts-per-Million Hydrogen Sulfide Colorimetric

Sensor: Lead Acetate Anchored Nanofibers toward Halitosis Diagnosis. *Analytical Chemistry* 2018, 90 (15): 8769-8775.

[26] Montoya LA, Pearce TF, Hansen RJ, Zakharov LN, Pluth MD: Development of Selective Colorimetric Probes for Hydrogen Sulfide Based on Nucleophilic Aromatic Substitution. *The Journal of Organic Chemistry* 2013, 78 (13): 6550-6557.

[27] Zhang J, Zhen X, Zeng J, Pu K: A Dual-Modal Molecular Probe for Near-Infrared Fluorescence and Photoacoustic Imaging of Peroxynitrite. *Analytical Chemistry* 2018, 90 (15): 9301-9307.

[28] Zhang J, Cheng P, Pu K: Recent Advances of Molecular Optical Probes in Imaging of β-Galactosidase. *Bioconjugate Chemistry* 2019, 30 (8): 2089-2101.

[29] Zhang J, Ning L, Huang J, Zhang C, Pu K: Activatable Molecular Agents for Cancer Theranostics. *Chemical Science* 2020, 11: 618-630.

[30] Yuan F, Li Y, Chen Z, Zhang J, Ning L, Yang X, et al.: Excimer-based Activatable Fluorescent Sensor for Sensitive Detection of Alkaline Phosphatase. *Chemical Research in Chinese Universities* 2021, 37 (4): 960-966.

[31] Miao Q, Xie C, Zhen X, Lyu Y, Duan H, Liu X, et al.: Molecular Afterglow Imaging with Bright, Biodegradable Polymer Nanoparticles. *Nature Biotechnology* 2017, 35 (11): 1102-1110.

[32] Liu Y, Xu C, Liu H, Teng L, Huan S, Yuan L, et al.: Precipitated Fluorophore-Based Molecular Probe for In Situ Imaging of Aminopeptidase N in Living Cells and Tumors. *Analytical Chemistry* 2021, 93 (16): 6463-6471.

[33] Zhang W, Huo F, Yue Y, Zhang Y, Chao J, Cheng F, et al.: Heat Stroke in Cell Tissues Related to Sulfur Dioxide Level is Precisely Monitored by Light-Controlled Fluorescent Probes. *Journal of the American Chemical Society* 2020, 142 (6): 3262-3268.

[34] Hou J, Wang B, Zou Y, Fan P, Chang X, Cao X, et al.: Molecular Fluorescent Probes for Imaging and Evaluation of Hypochlorite Fluctuations during Diagnosis and Therapy of Osteoarthritis in Cells and in a Mouse Model. *ACS Sensors* 2020, 5 (7): 1949-1958.

[35] Feng H, Meng Q, Ta HT, Zhang R: Development of "Dual-Key-and-Lock" Responsive Probes for Biosensing and Imaging. *New Journal of Chemistry* 2020, 44 (30): 12890-12896.

[36] Gao Y, Hu Y, Liu Q, Li X, Li X, Kim C, et al.: Two-Dimensional Design Strategy to Construct Smart Fluorescent Probes for the Precise Tracking of Senescence. *Angewandte Chemie International Edition* 2021, 60 (19): 10756-10765.

[37] Tian J, Shi D, Zhang Y, Li X, Li X, Teng H, et al.: Stress Response Decay with Aging Visualized using a Dual-Channel Logic-Based Fluorescent Probe. *Chemical Science* 2021, 12 (40): 13483-13491.

[38] Qian Y, Zhang L, Ding S, Deng X, He C, Zheng XE, et al.: A fluorescent probe for rapid detection of hydrogen sulfide in blood plasma and brain tissues in mice. *Chemical Science* 2012, 3 (10): 2920-2923.

[39] Zhang L, Zheng XE, Zou F, Shang Y, Meng W, Lai E, et al.: A highly selective and sensitive near-infrared fluorescent probe for imaging of hydrogen sulphide in living cells and mice. *Scientific Reports* 2016, 6 (1): 18868.

[40] Zhang L, Li S, Hong M, Xu Y, Wang S, Liu Y, et al.: A colorimetric and ratiometric fluorescent probe for the imaging of endogenous hydrogen sulphide in living cells and sulphide determination in mouse hippocampus. *Organic & Biomolecular Chemistry* 2014, 12 (28): 5115-5125.

[41] Zhao Y, Bolton SG, Pluth MD: Light-Activated COS/H_2S Donation from Photocaged Thiocarbamates. *Organic Letters* 2017, 19 (9): 2278-2281.

[42] Fukushima N, Ieda N, Kawaguchi M, Sasakura K, Nagano T, Hanaoka K, et al.: Development of

DOI: 10.55415/deep-2022-0055.v1

Photo-controllable Hydrogen Sulfide Donor Applicable in Live Cells. *Bioorganic & Medicinal Chemistry Letters* 2015, 25 (2): 175-178.

[43] Štacko P, Muchová L, Vítek L, Klán P: Visible to NIR Light Photoactivation of Hydrogen Sulfide for Biological Targeting. *Organic Letters* 2018, 20 (16): 4907-4911.

[44] Kang J, Li Z, Organ CL, Park C, Yang C, Pacheco A, et al.: pH-Controlled Hydrogen Sulfide Release for Myocardial Ischemia-Reperfusion Injury. *Journal of the American Chemical Society* 2016, 138 (20): 6336-6339.

[45] Yang C, Lai Z, Zheng Z, Kang J, Xian M, Wang R, et al.: A Novel pH-Controlled Hydrogen Sulfide Donor Protects Gastric Mucosa from Aspirin-Induced Injury. *Journal of Cellular and Molecular Medicine* 2017, 21 (10): 2441-2451.

[46] Chauhan P, Bora P, Ravikumar G, Jos S, Chakrapani H: Esterase Activated Carbonyl Sulfide/Hydrogen Sulfide (H_2S) Donors. *Organic Letters* 2017, 19 (1): 62-65.

[47] Steiger AK, Marcatti M, Szabo C, Szczesny B, Pluth MD: Inhibition of Mitochondrial Bioenergetics by Esterase-Triggered COS/H_2S Donors. *ACS Chemical Biology* 2017, 12 (8): 2117-2123.

[48] Liang D, Wu H, Wong MW, Huang D: Diallyl Trisulfide Is a Fast H_2S Donor, but Diallyl Disulfide Is a Slow One: The Reaction Pathways and Intermediates of Glutathione with Polysulfides. *Organic Letters* 2015, 17 (17): 4196-4199.

[49] Martelli A, Testai L, Citi V, Marino A, Pugliesi I, Barresi E, et al.: Arylthioamides as H_2S Donors: L-Cysteine-Activated Releasing Properties and Vascular Effects in Vitro and in Vivo. *ACS Medicinal Chemistry Letters* 2013, 4 (10): 904-908.

[50] Mahato SK, Bhattacherjee D, Bhabak KP: The biothiol-triggered organotrisulfide-based self-immolative fluorogenic donors of hydrogen sulfide enable lysosomal trafficking. *Chemical Communications* 2020, 56 (56): 7769-7772.

[51] Garcia AC, Zakharov LN, Pluth MD: Supramolecular Activation of S8 by Cucurbiturils in Water and Mechanism of Reduction to H2S by Thiols: Insights into Biological Sulfane Sulfur Trafficking. *Journal of the American Chemical Society* 2022, 144 (33): 15324-15332.

[52] Zhang N, Hu P, Wang Y, Tang Q, Zheng Q, Wang Z, et al.: A Reactive Oxygen Species (ROS) Activated Hydrogen Sulfide (H_2S) Donor with Self-Reporting Fluorescence. *ACS Sensors* 2020, 5 (2): 319-326.

[53] Chauhan P, Jos S, Chakrapani H: Reactive Oxygen Species-Triggered Tunable Hydrogen Sulfide Release. *Organic Letters* 2018, 20 (13): 3766-3770.

[54] Zhao X, Ning L, Zhou X, Song Z, Zhang J, Guan F, et al.: An Activatable Near-Infrared Fluorescence Hydrogen Sulfide (H_2S) Donor for Imaging H_2S Release and Inhibiting Inflammation in Cells. *Analytical Chemistry* 2021, 93 (11): 4894-4901.

[55] Zhang J, Wang J, Liu J, Ning L, Zhu X, Yu B, et al.: Near-Infrared and Naked-Eye Fluorescence Probe for Direct and Highly Selective Detection of Cysteine and Its Application in Living Cells. *Analytical Chemistry* 2015, 87 (9): 4856-4863.

[56] Levinn CM, Cerda MM, Pluth MD: Development and Application of Carbonyl Sulfide-Based Donors for H_2S Delivery. *Accounts of Chemical Research* 2019, 52 (9): 2723-2731.

[57] Chen B, Li W, Lv C, Zhao M, Jin H, Jin H, et al.: Fluorescent Probe for Highly Selective and Sensitive Detection of Hydrogen Sulfide in Living Cells and Cardiac Tissues. *Analyst* 2013, 138 (3): 946-951.

[58] Moest RR: Hydrogen Sulfide Determination by the Methylene Blue Method. *Analytical Chemistry*

DOI: 10.55415/deep-2022-0055.v1

1975, 47 (7): 1204-1205.

[59] Zheng Y, Yu B, De La Cruz LK, Roy Choudhury M, Anifowose A, Wang B: Toward Hydrogen Sulfide Based Therapeutics: Critical Drug Delivery and Developability Issues. *Medicinal Research Reviews* 2018, 38 (1): 57-100.

[60] Zhang J, Li C, Zhang R, Zhang F, Liu W, Liu X, et al.: A Phosphinate-Based Near-Infrared Fluorescence Probe for Imaging the Superoxide Radical Anion In Vitro and In Vivo. *Chemical Communications* 2016, 52 (13): 2679-2682.

[61] Bhatia M, Gaddam RR: Hydrogen Sulfide in Inflammation: A Novel Mediator and Therapeutic Target. *Antioxidants & Redox Signaling* 2021, 34 (17): 1368-1377.

[62] Karin M: NF-κB as A Critical Link Between Inflammation and Cancer. *Cold Spring Harbor Perspectives in Biology* 2009, 1 (5): a000141.

[63] Pinto RV, Carvalho S, Antunes F, Pires J, Pinto ML: Emerging Nitric Oxide and Hydrogen Sulfide Releasing Carriers for Skin Wound Healing Therapy. *ChemMedChem* 2022, 17 (1): e202100429.

[64] Xu M, Hua Y, Qi Y, Meng G, Yang S: Exogenous Hydrogen Sulphide Supplement Accelerates Skin Wound Healing via Oxidative Stress Inhibition and Vascular Endothelial Growth Factor Enhancement. *Experimental Dermatology* 2019, 28 (7): 776-785.

DOI: 10.55415/deep-2022-0055.v1

Graphical abstract

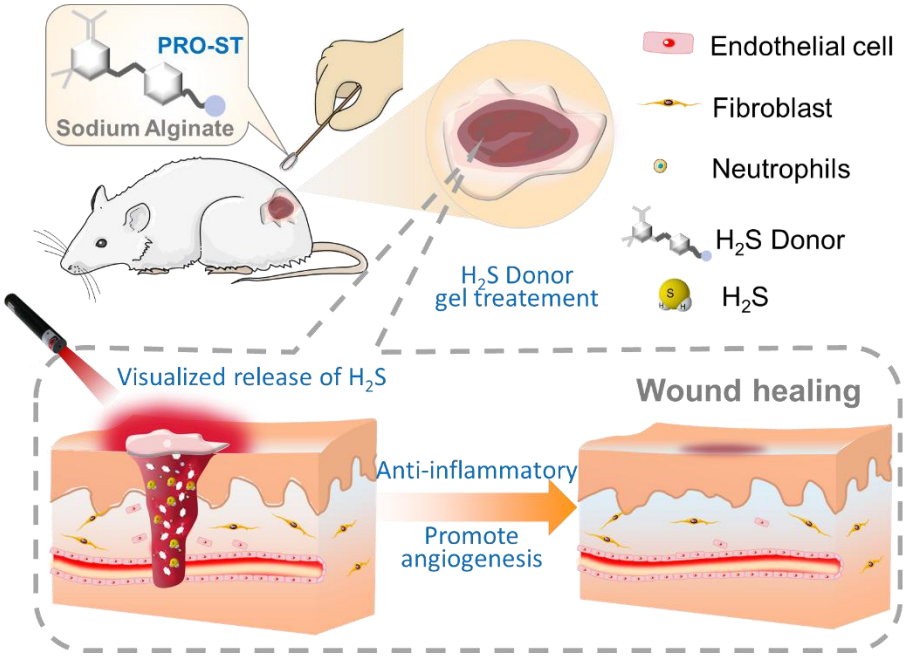

Authors

Xinyue Zhao, Mengbin Ding, Lulu Ning, Fang Yuan, Jingchao Li, Yuan Guo, Yuguang Mu, and Jianjian Zhang

Correspondence

zhangjj@nwu.edu.cn (J. Zhang)

Highlights

• **PRO-ST** exhibits strong NIR fluorescence enhancement (45-fold), prominent controllable H_2S release (60 min), high H_2S release efficiency (73%), and excellent cell compatibility.

• **PRO-ST** was activated by multiple biothiol stimulants to avoid the excessive consumption of a single stimulant which affects the local redox balance

• **PRO-ST** showed excellent real-time anti-inflammatory and *in-situ* visual promoting wound healing abilities in biological systems.

In brief

DOI: 10.55415/deep-2022-0055.v1

A biothiol-activated near-infrared (NIR) fluorescence hydrogen sulfide (H_2S) donor **PRO-ST** for real-time visualization of H_2S release was synthesized. **PPR-ST** can be used as a promising lead donor for real-time anti-inflammatory and wound healing promotion in biological systems.